

The Quasi-Normal Direction (QND) Method: An Efficient Method for Finding the Pareto Frontier in Multi-Objective Optimization Problems

Armin Ghane Kanafi*

Department of Mathematics, Lahijan Branch, Islamic Azad University, Lahijan, Iran

(Received: November 5, 2018; Revised: November 13, 2018; Accepted: April 7, 2019)

Abstract

In managerial and economic applications, there appear problems in which the goal is to simultaneously optimize several criteria functions (CFs). However, since the CFs are in conflict with each other in such cases, there is not a feasible point available at which all CFs could be optimized simultaneously. Thus, in such cases, a set of points, referred to as 'non-dominate' points (NDPs), will be encountered that are ineffective in relation to each other. In order to find such NDPs, many methods including the scalarization techniques have been proposed, each with their advantages and disadvantages. A comprehensive approach with scalarization perspective is the PS method of Pascoletti and Serafini. The PS method uses the two parameters of $a \in R^p$, $p \geq 2$ as the starting point and $r \in R^p$, $r \neq 0_p$ as the direction of motion to find the NDPs on the 'non-dominate' frontier (NDF). In bi-objective cases, the point $a \in R^2$ is selected on a special line, and changing point on this line leads to finding all the NDPs. Generalization of this approach is very difficult to three- or more-criteria optimization problems because any closed pointed cone in a three- or more-dimensional space is not like a two-dimensional space of a polygonal cone. Moreover, even for multifaceted cones, the method cannot be generalized, and inevitably weaker constraints must be used in the assumptions of the method. In order to overcome such problems of the PS method, instead of a hyperplane (two-dimensional line), a hypersphere is applied in the current paper, and the parameter $a \in R^p$ is changed over its boundary. The generalization of the new method for more than two criteria problems is simply carried out, and the examples, provided along with their comparisons with methods such as mNBI and NC, ensure the efficiency of the method. A case study in the realm of health care management (HCM) including two conflicting CFs with special constraints is also presented as an exemplar application of the proposed method.

Keywords

Multi-criteria optimization problems, Pareto surface, Non-convex and Nonlinear optimization, Health care management problem, Scalarization techniques.

*Author's Email: arminghane@liau.ac.ir

Introduction

Finding NDPs in multi-criteria optimization problems (MCOPs) has been one of the interesting topics in optimization issues, which has also been one of the earliest problems referred to in domains such as engineering design, resources optimization, and management science, etc. whose main objective is finding a collection of preferred answers of which a decision maker (DM) chooses an answer in order to reach the utmost benefits from the available resources. However, MCOP is the process of optimizing more than two CFs that are subject to certain constraints. Moreover, complicated communication in the feasible objective space (FOS) is involved. In the realm of MCOP there exist multiple contradictory objectives for which there is a collection of NDPs, which represent the interaction between the CFs. However, due to the plethora of function evaluations, it is neither wise nor economical to produce the entire NDF in experimental cases. Thus, in applied problems, we seek to reach a simple representation of NDPs.

Looking into the literature of research reveals that many studies have tried to detect NDPs. In this way, Uilhoorn (2017) presented an approach for constructing the NDPs of noise statistics for Kalman filtering, applied to the state estimation of gas dynamics. Moreover, Kasimbeyli, et al., (2017) performed a comparison of some approaches in MCOPs. Also, Lopeza, et al., (2013) presented a new MCO algorithm for non-convex non-dominance surfaces of CFs. Works by Abo-Sinna, et al., (2014), Audet, et al., (2008), Siddiqui, et al., (2011), Valipour, et al., (2014) and Pardalos, et al., (2017) are a number of other studies done to develop methods to approximate the NDF.

This paper focuses on Pascoletti and Serafini scalarization (PS) method (Eichfelder, 2008), and based on it, a numerical method to approximate the NDF of general MCOPs is presented. PS scalarization offers a number of advantages, the paramount one being the fact that it is general and many other scalarization methods are special cases from it (Eichfelder, 2008).

However, the PS method has two major problems. One problem is the generalization of the method to solve three- or more-objective optimization problems, and the other is that this method does not provide any solution for finding proper NDPs. The current paper examines the first problem and uses a hypersphere instead of a hyperplane to overcome it. The frequent selection of the starting point $a \in R^p$ from the boundary of the hypersphere and moving in the

direction $r \in R^p - \{0_p\}$ leads to the production of all NDPs on the NDF. Then in the numerical examples section, the advantages of the introduced approach is shown in two numerical examples along with an application in the realm of the health care management (HCM) to treat prostate cancer (PC), and the validity of the results is measured by three qualitative criteria. The article is organized as follows.

In the second Part, the basic topics governing MCP and a brief explanation of the PS method are presented. The third part examines the qualitative criteria used in the paper, and then in section 4, the proposed method is examined in detail. An algorithm for implementing the proposed method and the theorems for validating the method are also presented in section 4. Examples and numerical simulations and study of HCM are provided in part 5, and finally, in the last part conclusions are presented.

Basic concepts

An MCOP with more than one conflicting criteria is given by

$$\begin{aligned} \text{MCOP: } \min \quad & f(x), p \geq 2 \\ \text{s.t.} \quad & x \in X \end{aligned} \tag{1}$$

Where $X = \{x \in R^n \mid g_i(x) \leq 0_s, h_j(x) = 0_l, \underline{x} \leq x \leq \bar{x}, \forall i, j\} \subseteq R^n$ and $f(x) = (f_1(x), \dots, f_p(x))^T$ are nonempty feasible set (FS) and CF, respectively. Also $f(x)$ represents the vector of objectives and $f_k, k = 1, \dots, p$ ($p \geq 2$) is a scalar function which is the image of the designer variable x into the FOS $f_k : R^n \rightarrow R, k = 1, \dots, p$. Because the criteria conflict with each other, no unique answer can simultaneously minimize all single objective functions (SOFs) $f_k(x), k = 1, \dots, p$. Therefore, it needs to introduce an efficiency notion, considered as an important evaluating criterion in economic and management sciences.

For two vectors $y, \hat{y} \in R^p$,

$y < \hat{y}$ is equivalent to $y_k < \hat{y}_k$ where in $k = 1, \dots, p$,

$y \leq \hat{y}$ is equivalent to $y_k \leq \hat{y}_k$ where in $k = 1, \dots, p$,

$y \leq \hat{y}$ is equivalent to $y \leq \hat{y}$ and $y \neq \hat{y}$.

In this article, the component arrangement above is used to order the

FOS and define the cone $R_{\geq}^n = \{x \in R^n | x \geq 0_n\}$.

Definition 2.1. For a p -objective problem, the point $f^{i*} = (f_1(x_i^*), \dots, f_p(x_i^*))^T$ in which $x_i^* = \arg \min_{x \in X} f_i(x)$ with $i = 1, \dots, p$, is called the i -th anchor point.

Definition 2.2. In the FOS the point $y^N = (y_1^N, \dots, y_p^N)^T$ in which $y_i^N = \max_{x \in X_E} f_i(x)$ with $i = 1, \dots, p$, is called the i -th component of nadir point.

It is notable that another useful way to define y_i^N is

$$y_i^N = \max \{f_i(x_1^*), \dots, f_i(x_p^*)\}, i = 1, \dots, p. \quad (2)$$

The other definition related to the Pareto solutions is given below:

Definition 2.3. A feasible point $\hat{x} \in X$ is called A weakly efficient solution (WES) of MCOP (1) if there is no other $x \in X$ in which $f(x) < f(\hat{x})$. If $\hat{x} \in X$ is WES, then $f(\hat{x})$ is called a weakly non-dominated point (WNDP).

An efficient solution (ES) of MCOP (1), if there is no other $x \in X$ in which $f(x) \leq f(\hat{x})$. If $x^* \in X$ is ES, then $f(x^*)$ is called a non-dominated point (NDP).

The collection of all ES and WES of MCOP (1) is represented by X_E and X_{wE} , respectively. This image is called by titles such as NDP and WNDP sets, which are denoted by Y_N and Y_{wN} , respectively.

Definition 2.4. The point $y^I = (y_1^I, \dots, y_p^I)$ is called the MCOP ideal point (1) where $y_i^I = \min_{x \in X} f_i(x)$, $i = 1, \dots, p$.

Now let's take a look at the PS approach in brief.

Notations r and a are the parameters of the PS scalarization which are selected from $R^p - \{0_p\}$ and R^p , respectively. The following model based on the ordering cone R_{\geq}^p can be solved in order to determine the ES of MCOP (1):

$$\begin{aligned} \min \quad & t, \\ \text{s.t.} \quad & a + tr \geq f(x), \\ & t \in R, x \in X \end{aligned} \quad (3)$$

To solve the model (3), the cone $-R_{\geq}^p$ is moved in the path of r or

$-r$ on the beam $a + tr$ which starts at the initial point a until the intersection of $(a + tr - R_{\leq}^p) \cap f(X)$ decreases to an empty collection. The smallest \bar{t} which causes the above set not to be empty is the minimal value of the scalarization optimization problem (3); see Figure.1 for a bi-criteria problem.

Theorem 2.1. (Eichfelder, 2009) Consider the closed pointed convex cone R_{\leq}^p .

a. Assume \bar{x} be an ES of MCOP (1), then $(0, \bar{x})$ is an optimal solution (OS) of (3) with $a = f(\bar{x})$ and arbitrary $r \neq 0_p$.

b. Assume (\bar{t}, \bar{x}) be an OS of (3), then \bar{x} is a WES of MCOP (1) and $a + \bar{t}r \geq f(\bar{x})$.

Theorem 2.2. (Eichfelder, 2009) Consider the closed pointed convex cone R_{\leq}^p . Let the set $f(X) + R_{\leq}^p$ be closed and convex, and let $Y_N \neq \emptyset$, then there exists a minimal solution of (3) for all parameters $(a, r) \in R^p \times R_{\leq}^p - \{0_p\}$.

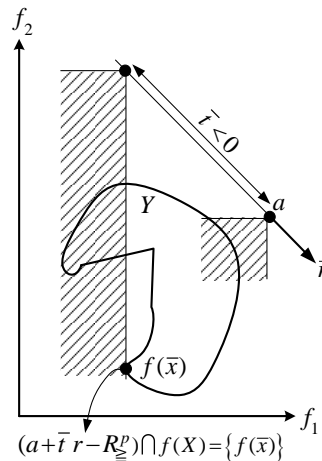


Figure 1. Visualization of the PS problem. Here, Y is the FOS.

As a consequence, if the problem (3) is solved for any choice of parameters $(a, r) \in R^p \times R_{\leq}^p - \{0_p\}$ with $f(X) + R_{\leq}^p$ closed and convex, and if there exists no minimal solution of (3), then $Y_N = \emptyset$.

In Eichfelder (2008), an approach is proposed to reduce the choice of a into R^p , which still obtains all the NDP for MCOPs with an ideal point.

For more than bi-criteria problems, the above approach has not any desirable result (see Example 2.19 in Eichfelder (2008), for further discussion).

The set $\bar{H} := \{y \in H \mid y + t r = f(x), x \in X, t \in R\} \subset H$ is defined as one which has an irregular boundary and because of this, is not appropriate to be considered in a systematic procedure. The approach of constructing H^0 is given in Eichfelder (2008), which is complex in practice to implement. As a result of the above explanation, this approach might be difficult to be verified in practice.

Contrary to the bi-criteria optimization problems, in the case of more than two objective functions, one cannot generalize such a hyperplane to problems with more than two CFs in the same way as the H -hyperplane on bi-objective problems. This problem originates from the fact that for finding any NDP on the NDF, it might not be possible to perceive a solution on the hyperplane H , assuming that the right direction of r leads to finding that NDP. To solve this problem, Pascoletti and Serafini had to use a weaker constraint to construct the H -hyperplane and choose the a point on it. The proposed method, which is discussed in Section 4, overcomes this problem with a clever technique, namely, using a hypersphere instead of the hyperplane.

The indicator of inclusion and distance

Now, to continue the previous discussion, important criteria are introduced for determining the measure of the modality of the allotment of approximation points.

Extension (EX) (Meng, et al., 2005)

An indicator of inclusion checks whether all areas of the efficient surface are displayed or not. One such measure of coverage, called "extension" (Meng, et al., 2005), is used in this paper. Suppose that $y^I = (y_1^I, \dots, y_p^I)^I$ in which y_i^I for $i = 1, \dots, p$ is the ideal point. The distance between each and every element of the ideal point from Y_N is denoted by $d(y_i^I, Y_N)$, assuming that there exists a discrete representation of Y_N

$$d(y_i^I, Y_N) = \min \{d(y_i^I, y) \mid y \in Y_N\} \quad (4)$$

Finally, the extension is as follows:

$$EX(Y_N) = \frac{\sqrt{\sum_{i=1}^p (d(y_i^I, Y_N))^2}}{p} \tag{5}$$

For the above equation, smaller values are more suitable; this is because large values might prompt the idea that the demonstration is located in the middle of the efficient curve, which neglects the surrounding points.

Evenness (ξ) (Messac and Mattson, 2004)

A collection of points is uniformly distributed over a region. If compared to other parts, no part of that region is flank represented in that set of points. An indicator of distribution evenness is described below.

The spacing value determines the distance between the represented points. It should be noted that reaching a uniform-spacing representation is desirable. However, the existence of a representation of points with the same distance does not provide acceptable inclusion necessarily. In the current article, the spacing scale which is called “evenness” (Messac and Mattson, 2004) is applied. Two hyper-spheres are produced for one and all point y^i in the separate demonstration, namely the smaller hyper-sphere that can be made between point y^i and each different point in the collection whose diameter is displayed by d_l^i , and a larger hyper-sphere which is constructed by diameter, d_u^i , which has the highest amount of distance between point y^i and each points in the set which leads to the fact that no point in the set is within the larger hyper-sphere. This way, the evenness measure is represented by the expression $\xi = \frac{\sigma_d}{\bar{d}}$, where \bar{d} and σ_d denote the mean and standard deviation of d , respectively, and where $d^i = \{d_l^i, d_u^i\}$ and $d = \{d^1, \dots, d^{2n_p}\}$. A collection of points is uniformly distributed when $\xi = 0$ because d_l^i and d_u^i are equal (i.e. $\sigma_d = 0$). In this paper and in the proposed QND approach, it is assumed that the criteria region is normalized, namely $0 \leq f_i \leq 1, \forall i \in \{1, \dots, p\}$. Note that the normalized value of the criteria region can be computed using the ideal and nadir points. For this, suppose that there are ideal and nadir points. This issue

is given in the equation below:

$$f_i \leftarrow f_i^{\text{nrI}} := \frac{f_i - y_i^I}{y_i^N - y_i^I} \quad (6)$$

where y^I and y^N are the ideal and nadir points, respectively. Here, the i -th component f_i^{nrI} is the normalized form of the single objective f_i for $i = 1, \dots, p$. In the next part, the proposed approach for solving the problem of the generalization of the PS method in more-than-one-objective optimization problems that provides an effective solution is discussed in detail.

Description of the quasi-normal direction method (QND)

As noted above, the proposed method by Pascoletti and Serafini (Eichfelder, 2008) has some limitations in practice. Construction of a hyperplane in which initial points are selected is simply not possible. So a weaker restriction is proposed for the parameter α of the set H , which is done through the projection of $f(X)$ towards r onto set H (Eichfelder, 2008). Here, another method is proposed, namely the QND approach, which does not have the foregoing limitation. The QND method uses a *posteriori* approach in which parameters which have an equidistance spread lead to the NDPs with an equidistance spread on the NDF. In Practice, this method acts in a similar way to the NBI and NC methods. Accessing a more even dispensation of the NDPs to improve the measures of coverage and spacing and improving the time of complexity compared with other methods is the foremost incentive behind the suggested approach in this article. It is worth noting that, the performance of most approaches in MCOPs is more or less dependent on the NDF geometry.

Consider the MCOP (1). It is assumed that the model (1) has an individual ideal solution. To determine this ideal solution as a reference point, the problem minimize $f(x)$ subject to $x \in X$ for $i = 1, \dots, p$ is solved. Assume that y_i^I be an optimal quantity of minimizing $f(x)$ subject to $x \in X$ for $i = 1, \dots, p$. The ideal solution is marked by the notation $y^I = (y_1^I, \dots, y_p^I)$. Then the objective functions should be normalized in order for all criteria functions to have a minimum and maximum at zero and one, respectively (see Equation 4).

In the remainder of this section, the ideal solution is considered to be

the origin; moreover, the CFs are considered non-negative. Then the collection

$$\Lambda = \left\{ \frac{v}{\|v\|_2} \mid v \in \mathbb{R}_{\geq}^p, \sum_{i=1}^p v_i = 1, v_i \geq 0, i = 1, \dots, p \right\} \quad (7)$$

is defined ($\|\cdot\|_2$ is the Euclidian norm). It is clear that this set is used as a starting point for achieving the NDF. The geometry of the Λ is shown in Figure. 2.

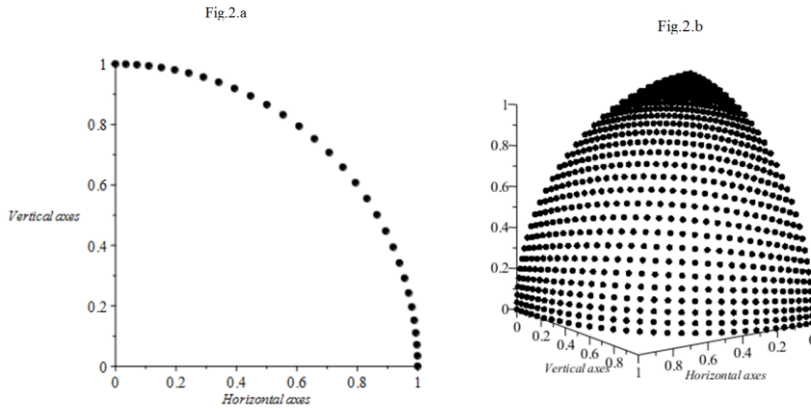


Figure 2. The set Λ with $\delta = \frac{1}{30}$ for bi-objective (Figure. 2.a) and three-objective problems. Figure. 2.b: respectively.

Assume that the (quasi) normal direction is equal to $\bar{n} = \Phi e$.

Now, consider the following set

$$Y = \{u \mid u = \hat{v} + t\bar{n} \text{ where } \hat{v} \in \Lambda, t \in \mathbb{R}, \bar{n} = \Phi e\} \quad (8)$$

In which Φ is the $p \times p$ pay-off matrix. Choose an arbitrary point, u_k into the set Y (utopia circle). Figure.3 illustrated the description of the QND method for bi-objective problems. Finding NDP on the NDF underlies the QND approach.

Thus, to produce the NDF, the following optimization problem must be solved

$$\begin{aligned} &\min t, \\ &s.t. \quad u - f(x) \in \mathbb{R}_{\geq}^p, \\ &\quad \quad u \in Y, x \in X. \end{aligned} \quad (9)$$

Problems such as (9) are solved through ordering cone $-\mathbb{R}_{\geq}^p$ towards \bar{n} or $-\bar{n}$ on the line $u \in Y$ that starts at $\hat{v} \in \Lambda$ to reduce the set

$(u - R_{\leq}^p) \cap f(X)$ to a blank collection for all $u \in Y$. The smallest value of t satisfied in (9) above is considered as an optimal value of such problems.

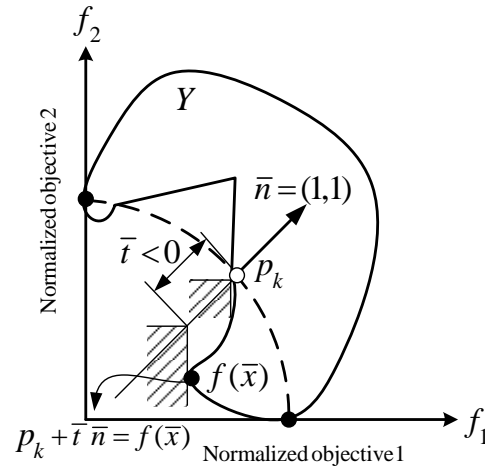


Figure 3. Graphical description of QND method for a bi-criteria optimization model. Here p_k is a generic point on the utopia circle and $\bar{n} = \Phi e = (1,1)$ is the quasi-normal direction.

Eichfelder (2008) proposed an approach to produce $p \in \Lambda$, which is considered to be an even distribution of combination vectors in which $0, \delta, 2\delta, \dots, 1$ are the values of different components for which $\delta = \frac{1}{n} < 1$ is a fixed step size and n is a non-negative integer.

The set Λ is considered as the first quarter of the unit circle in bi-objective problems (see Figure.2a); however, in problems with three objectives, Λ is considered as the first octant of the unit sphere (see Figure. 2b). As an iterative method, QND generates a set of points which are considered as approximations of the NDF, Y_N in which in each iteration the NDP is denoted by Y_A which presents an estimation of the real NDF, Y_N .

At first, the ideal point is found and normalized according to Equation 6. Also, set $Y_A = \emptyset$. The iterations in the QND algorithm include two stages which are as follows. Firstly, the direction $\bar{n} = \Phi e$ and the k -th point $p_k \in \Lambda$ on the hypersphere is used. Secondly, problem 9 is used by direction \bar{n} and the k -th point $p_k \in \Lambda$. In the second stage, therefore, the set of NDPs, Y_A will be updated at each iteration.

The general overview of the QND approach is presented below.

The QND Algorithm

Input: MCOP.

Output: Determine the approximate set of NDF denoted by Y_A .

The initial steps

- Determine the ideal point according to Definition 2.4.
- Normalize all objective functions according to Equation 6.
- Let $Y_A = \emptyset$.
- Determine m as the desired number of NDPs; set $\delta = \frac{1}{m}$ and define

$L = \{i\delta\}_{i=0}^m$ as the set of points on the CHIM.

- Define the set of initial points according to (7) and let the fixed (pseudo) normal direction be $\bar{n} = \Phi \mathbf{e}$. Let p_k be denoted as the k -th element of Λ , and $|\Lambda|$ be a cardinal number of the set of points Λ on the hypersphere. Set $k = 1$ and restate the procedure below to establish $k = |\Lambda|$.
-

The main steps

- Determine the initial point $p_k \in \Lambda$, and according to set Υ solve the single optimization problem (SOP), 9.
 - Update Y_A : Actually, Y_A contains all NDPs in the current repetition. Set $k := k + 1$ and repeat the procedure until the stop criterion is established. In this step, the obtained NDP collection Y_A is an approximate of the true NDP set Y_N .
-

Justification of this two-step approach is shown thorough WES of (9).

Theorem 4.1. Consider \bar{x} as a WES of the model (1). Now prove that for arbitrary $\bar{n} \in \text{int}(R_{\geq}^p)$, $(0, \bar{x})$ can be an OS of the parameter $p := f(\bar{x}) \in \Lambda$ of the problem (9).

Proof. Set $p := f(\bar{x})$ and choose $\bar{n} \in \text{int}(R_{\geq}^p)$ as arbitrary. Then the point $(0, \bar{x})$ is feasible for problem (9) because

$$\mathbf{p} + t\bar{n} = f(\bar{x}) + 0 \cdot \bar{n} \geq f(\bar{x}).$$

The above solution is possible for problem (1) since based on considering theorem \bar{x} as a WES of model (1), therefore, $\bar{x} \in X$. Moreover the solution $(0, \bar{x})$ is considered an OS of (9); differently, there will be a possible solution (t', x') with $t' < 0$ and a $k' \in R_{\geq}^p$ with

$$p + t' \bar{n} - f(x') = k' \in R_{\geq}^p.$$

Therefore, this conduces to $f(\bar{x}) = f(x') + k' - t' \bar{n}$ which is $k' - t' \bar{n} \in \text{int}(R_{\geq}^p)$ that leads to $f(\bar{x}) \geq f(x')$ which is incongruent with the WSE of the MOP (1), namely \bar{x} .

Theorem 4.2. Let \bar{x} be an ES of the model (1), then $(0, \bar{x})$ is an optimal answer of (9) for the $p := f(\bar{x})$ and $\bar{n} \in R_{\geq}^p \setminus \{0_p\}$.

Proof. From the previous theorem, it is clear that the solution $(0, \bar{x})$ is a possible solution for the model (9). Even, it is an OS; otherwise, there is another point (t', x') and a scalar $t' < 0$ and $k' \in R_{\geq}^p$ with

$$p + t' \bar{n} - f(x') = k' \in R_{\geq}^p.$$

For this reason, $f(\bar{x}) = f(x') + k' - t' \bar{n}$. It is $k' - t' \bar{n} \in R_{\geq}^p$, and

$$f(\bar{x}) \in f(x') + R_{\geq}^p.$$

Since \bar{x} is an ES to the model (9), then it is concluded that $f(\bar{x}) = f(x')$, and thus $k' = t' \bar{n}$.

Since R_{\geq}^p is a pointed-cone, $k' \in R_{\geq}^p$ and $t' \bar{n} \in -R_{\geq}^p$; this implies $t' \bar{n} = k' = 0$. Thus, it is incongruity with $t' < 0$ and $\bar{n} \neq 0$.

Theorem 4.3. Assume (\bar{t}, \bar{x}) is an OS of (9). Then \bar{x} is a WES of the model (1).

Proof. Let \bar{x} be not WES. Then there is another point $x' \in X$ and a $k' \in \text{int}(R_{\geq}^p)$ with $f(\bar{x}) = f(x') + k'$.

As (\bar{t}, \bar{x}) is an OS of (9) and hence feasible for (9) there is a $\bar{k} \in R_{\geq}^p$ with $p + \bar{t} \bar{n} - f(\bar{x}) = \bar{k}$.

Because $k' \in \text{int}(R_{\geq}^p)$ and $\bar{k} \in R_{\geq}^p$ implies $k' + \bar{k} \in \text{int}(R_{\geq}^p)$, there is a $\varepsilon > 0$ with $k' + \bar{k} - \varepsilon \bar{n} \in \text{int}(R_{\geq}^p)$.

Then it is concluded that from $p + \bar{t} \bar{n} - f(x') - k' = \bar{k}$,

$$p + (\bar{t} - \varepsilon) \bar{n} - f(x') \in \text{int}(R_{\geq}^p).$$

Then the point $(\bar{t} - \varepsilon, x')$ is possible for (9) too, with $\bar{t} - \varepsilon < \bar{t}$ incongruity to (\bar{t}, \bar{x}) being the OS of (9).

Theorem 4.4. A solution (\bar{t}, \bar{x}) is an OS of the problem (9), with $\bar{n} = \Phi \mathbf{e}$ and $\hat{p} \in \Lambda$, if and only if (\bar{t}, \bar{x}) is an OS of problem PS(a, r).

In the next section, the effectiveness of the suggested method is examined in a number of examples, and the quality of the responses is measured using the qualitative criteria examined in Section 3.

Numerical examples

In this section, two examples from Deb (2001) and Zhang, et al. (2008) and one example from the HCM of PC treatment (Craft, et al., 2007) are used to display the accuracy and performance of the QND approach. For all test problems, the results obtained by QND are compared with the results from the mNBI approach (Shukla, 2007) and the NC approach (Messac, et al., 2003). Through applying the *Global Solve* solver of the *Global Optimization* package in Maple 2018, all single-objective optimization problems (SOPs) of the current paper are solved. The algorithm in the *Global Optimization* Toolbox is known as a global search method (Pintér, et al. 2006).

Bi-objective problems

In this subsection, the test problem F5 is considered from Zhang, et al., (2008).

Unconstraint problem (F5 in Zhang, et al., 2008)

The bi-objective to be minimized:

$$\begin{aligned} \min f_1(x) &= x_1 + \frac{2}{|J_1|} \sum_{j \in J_1} y_j^2, \\ \min f_2(x) &= 1 - \sqrt{x_1} + \frac{2}{|J_2|} \sum_{j \in J_2} y_j^2, \\ \text{s.t. } & 0 \leq x_1 \leq 1, -1 \leq x_j \leq 1, j = 2, \dots, n. \end{aligned} \tag{10}$$

where

$$J_1 = \{j | j=2k-1, 2 \leq j \leq n, k \in N\}, J_2 = \{j | j=2k, 2 \leq j \leq n, k \in N\}$$

and

$$y_j = \begin{cases} x_j - \left[0.3x_1^2 \cos(24\pi x_1 + \frac{4j\pi}{n}) + 0.6x_1 \right] \cos(6\pi x_1 + \frac{j\pi}{n}) & , j \in J_1 \\ x_j - \left[0.3x_1^2 \cos(24\pi x_1 + \frac{4j\pi}{n}) + 0.6x_1 \right] \cos(6\pi x_1 + \frac{j\pi}{n}) & , j \in J_2 \end{cases}$$

The FS is $[0,1] \times [-1,1]^{n-1}$.

Its NDF is $f_2 = 1 - \sqrt{f_1}$, $0 \leq f_1 \leq 1$ and its ES set is

$$x_j = \begin{cases} \left[0.3x_1^2 \cos(24\pi x_1 + \frac{4j\pi}{n}) + 0.6x_1 \right] \cos(6\pi x_1 + \frac{j\pi}{n}) & , j \in J_1 \\ \left[0.3x_1^2 \cos(24\pi x_1 + \frac{4j\pi}{n}) + 0.6x_1 \right] \cos(6\pi x_1 + \frac{j\pi}{n}) & , j \in J_2 \end{cases}$$

Assume $n = 4$. The problem is solved by QND, the mNBI and NC methods with $\delta = \frac{1}{100}$. The real NDF and the efficient frontier (EF) in the 3D feasible region are demonstrated in Figure.4.

The comparative results of the QND, mNBI, and NC methods for finding 101 Pareto optimal points after 96226264, 39992166845 and 10567553 total function evaluations (TFE) for the current problem are illustrated in Figures.5-7, respectively. Details are given in Table 1.

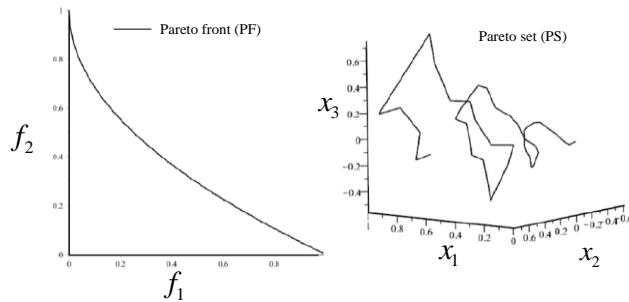


Figure 4. Representation of the NDF and the EEF in FS of instance F5 test problem.

Table 1. Run time (s), TFE rate, coverage measure (EX) and Density (ξ), and the dominance between solutions of the QND, mNBI, and NC methods for F5 problem (Zhang et al., 2008).

| Method | F5 test problem | | | |
|--------|-----------------|-----------|-----------|-----------|
| | Run time (s) | TFE | EX | ξ |
| QND | 3332.150 | 96226264 | 0.0038039 | 0.0036968 |
| mNBI | 15253.542 | 399216845 | 0.0038039 | 0.0063251 |
| NC | 585.784 | 10567553 | 0.0038039 | 0.0046713 |

Solutions of the QND dominate 171 solutions of the mNBI.
 Solutions of the mNBI dominate 94 solutions of the QND.
 Solutions of the QND dominate 210 solutions of the NC.
 Solutions of the NC dominate 183 solutions of the QND.
 Solutions of the mNBI dominate 144 solutions of the NC.
 Solutions of the NC dominate 125 solutions of the mNBI.

Responses achieved by QND approach dominated 171 and 210 answers achieved by mNBI and NC approaches of 10201 comparisons, respectively. Also, from this number of comparisons, answers achieved by mNBI and NC approaches dominated 94 and 183 solutions obtained by the QND method. Comparing EX and ξ in the three above-mentioned methods yields the fact that the approximation points' distribution quality of the QND method is more desirable than that of mNBI and NC approaches.

A comparison of Figure.5-7 and Table 1 display that the approximation points' distribution quality of the QND method is more suitable than those of the mNBI and NC methods.

Three-objective problems

The three-objectives to be minimized:

$$\begin{aligned} \min f_1(x) &= x_1, \\ \min f_2(x) &= x_2, \\ \min f_3(x) &= (1 + g(x)) \left(3 - \sum_{i=1}^2 \left(\frac{x_i}{1 + g(x)} (1 + \sin(3\pi x_i)) \right) \right), \quad (11) \\ \text{s.t. } x_i &\in [0, 1], i = 1, 2, \dots, 22, \\ g(x) &= 1 + \frac{9}{20} \sum_{i=3}^{22} x_i. \end{aligned}$$

The efficient set is separated into four non-connected sections. The set of ES is a subset of the set

$$\{x \in R^{22} | x_i = 0, i = 3, \dots, 22\}$$

and therefore the non-dominated set is a subset of the set

$$Y = \left\{ y \in R^3 \left| y_1, y_2 \in [0, 1], y_3 = 2 \left(3 - \sum_{i=1}^2 \frac{y_i}{2} (1 + \sin(3\pi y_i)) \right) \right. \right\}$$

which is plotted in Figure.8. The problem is solved by the QND, the mNBI, and NC methods with $\delta = \frac{1}{15}$ for producing 256 NDPs on the real NDF.

The convergence to the NDF and also the distribution of solutions of the QND, mNBI, and NC methods for finding 256, NDP after 103109965, 121624414 and 87449325 TFE for the current problem are illustrated in Figures.9-11, respectively. Results of the proposed method are listed in Table 2.

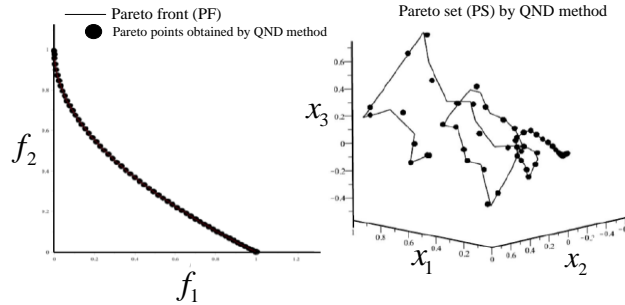


Figure 5. The QND method with 96226264 TFEs, for instance, F5 test problem (Zhang, et al., 2008).

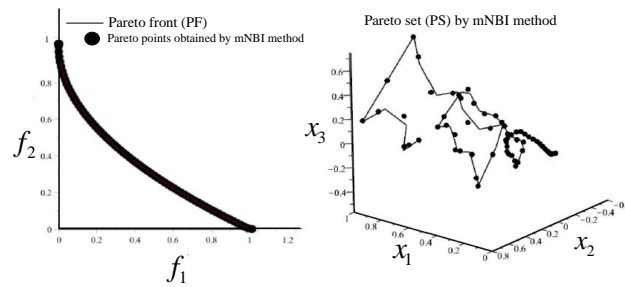


Figure 6. The mNBI method with 399216845 TFEs, for instance, F5 test problem (Zhang, et al., 2008).

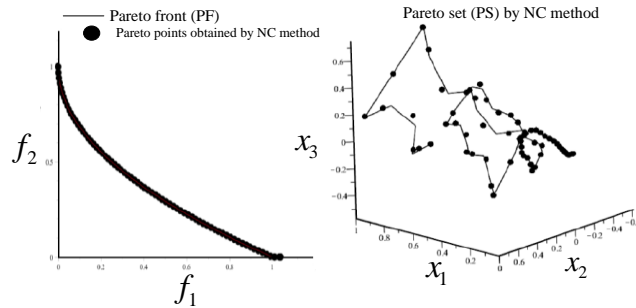


Figure 7. The NC method with 10567553 TFEs, for instance, F5 test problem (Zhang, et al., 2008).

Answers achieved by QND approach dominated 152 and 183 answers obtained by the mNBI and NC. Also, from this number of comparisons, answers achieved by the mNBI and NC approaches dominated 94 and 138 solutions obtained by the QND method.

Table 2 demonstrates that the solution distributions of the QND method are better than those of the mNBI and NC methods.

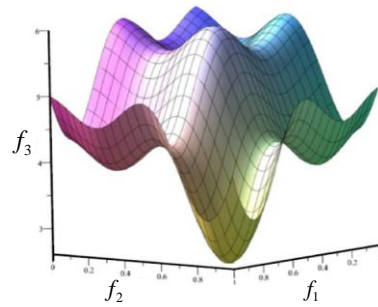


Figure 8: Illustration of the set Y .

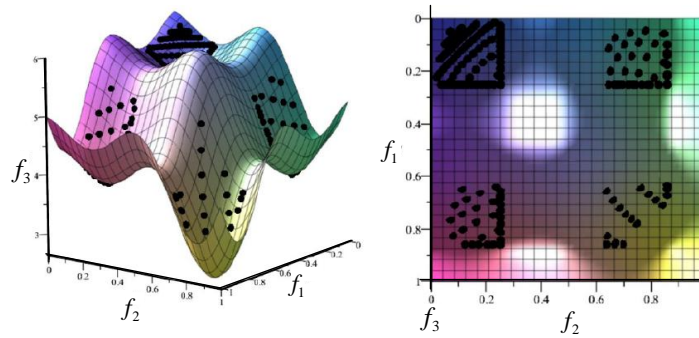


Figure 9. The QND method with 103109965 TFEs.

Table 2. Run time (s), TFE rate, coverage measure (EX) and Density (ξ), and the dominance between solutions of the QND, mNBI, and NC methods.

| Method | Three-objective test problem | | | |
|--------|------------------------------|-----------|-----------|-----------|
| | Run time (s) | TFE | EX | ξ |
| QND | 4759.544 | 103109965 | 0.0016829 | 0.0096630 |
| mNBI | 4303.678 | 121624414 | 0.0018468 | 0.0172651 |
| NC | 9438.544 | 87449325 | 0.0019468 | 0.0144486 |

Solutions of the QND dominate 152 solutions of the mNBI.
 Solutions of the mNBI dominate 94 solutions of the QND.
 Solutions of the QND dominate 183 solutions of the NC.
 Solutions of the NC dominate 138 solutions of the QND.
 Solutions of the mNBI dominate 80 solutions of the NC.
 Solutions of the NC dominate 175 solutions of the mNBI.

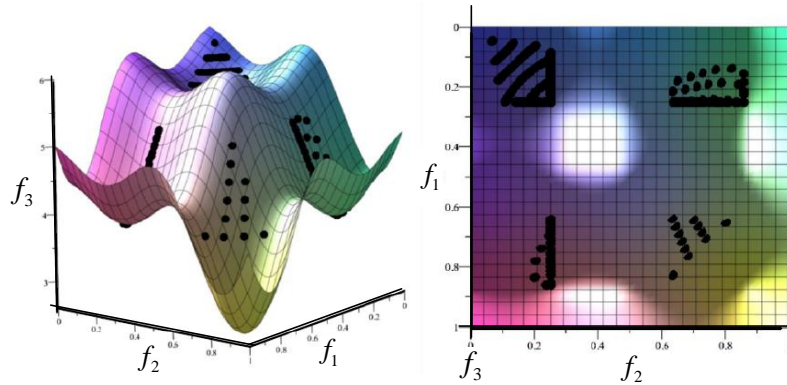


Figure 10. The mNBI method with 121624414 TFEs.

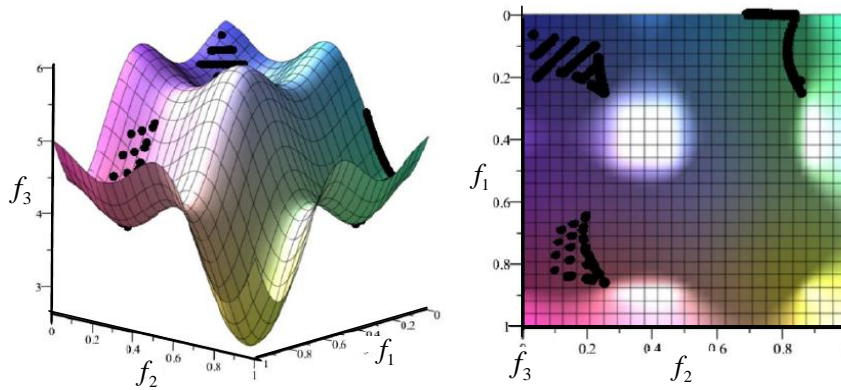


Figure 11. The NC method with 87449325 TFEs.

Application to HCM for IMRT treatment planning (Craft, et al., 2007)

As is proposed in the introduction of the current manuscript, there are a number of multi-criteria structure problems in engineering, economic and management applications which are often viewed as an SOP. An example of this is found in IMRT in which the main goal of the doctor is to destroy or reduce the tumor and at the same time to leave the surrounding healthy tissues untouched (see Alber and Reemtsen, 2007; Cotrutz, et al., 2001; Ehrgott and Burjony, 2001, for discussion). IMRT is multi-objective; that is to say, for this problem there exist more than one competing criteria which must be optimized at the same time.

For this paper, the QND algorithm proposed in the current manuscript has been applied to solve such bi-objective problems of PC.

With an available solution set as such, the therapist can juxtapose the criteria values of several answers and base the resulted decisions on knowledge. According to Eichfelder (2014), the cancer tumor can be radiated by five streams with equal distances, which includes a compilation of 400 distinctly suppressible pencil beams. If the radiation structure is immovable and the researcher concentrates on an optimization of the radiation strength, that part of the patient's body affected by the beams can be sketched by a system. According to the thickness of the slivers of the CT-slices in such experiments, the body of the patient is anatomized in voxels $v_j, j=1, \dots, 25787$. As the researcher might face a lot of voxels, he can reduce this by applying a clustering method proposed by Küfer, et al. (2003) that results in 8577 clusters. This has the same radiation stress with respect to a one-radiation unit. Such clusters are denoted as c_1, \dots, c_{8577} . As is indicated in figure 12 below, in the case study of the current manuscript, B_0, B_1 represent the tumor, B_2 represents the rectum, B_3 and B_4 represent the hip-bones in both sides of the body, respectively, B_5 represents the other tissues, and finally B_6 represents the bladder.

Küfer et al. (2003) proposed that under radiation, B_6 and B_2 are the most susceptible organs in receiving the radiation doses. Moreover, the sparing of B_6 leads to a high dose B_2 and vice versa. The emission of the stream $B_i, i \in \{1, \dots, 200\}$ to the clusters $c_j, j \in \{1, \dots, 8577\}$ demonstrated by the matrix $A = (a_{ji})_{8577 \times 200}$. Let $x \in R^{200}$ be the strong form of the stream. Then, $A_j x$ with A_j the j th row of the matrix A depicts the radiation dosage in the c_j , caused by the stream B_i , for the behavior scheme x . According to Brahme (1984), in order to compare the radiation stress in the organs, the researcher has to use the EUD.

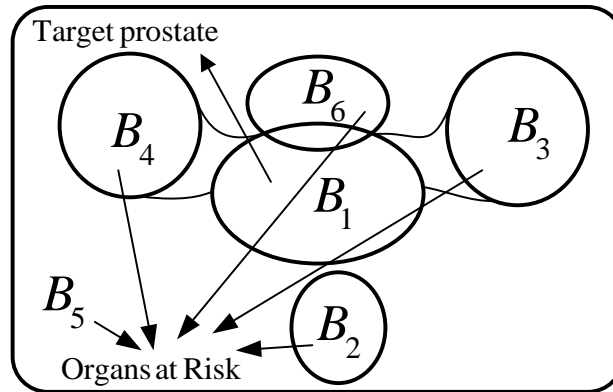


Figure 12. Schematic axial body cut.

According to Niemierko’s EUD (Niemierko, 1997) and using p -norm such as clustered voxels, the following formula can be considered:

$$D_k(x) = A_k \sqrt[k]{\frac{1}{|B_k|} \sum_{\{j|c_j \in B_k\}} |c_j| \cdot (A_j x)^{A_k}}, k = 2, \dots, 6 \quad (12)$$

The disparity of the variable dose in a part from the appropriated perimeter U_k is counted by $L_k(x) = \frac{1}{U_k} D_k(x) - 1$. The number of voxels in the organ B_k and cluster c_j are demonstrated by $|V_k|$ and $|c_j|$, respectively. It is notable that $\sum_{\{j|c_j \in B_k\}} |c_j| = |B_k|$. The results of the case study of the current manuscript are presented in Table 3 below. The main purpose of the current study is reduced B_2 and B_6 .

In this case, we will have the following bi-objective problem:

$$\begin{aligned} & \min L_6(x), \\ & \min L_2(x) \\ & s.t. \quad U_k(L_k(x)+1) \leq Q_k, k \in \{2, \dots, 6\} \\ & \quad \alpha_0(1-\gamma_0) \leq A_j x \leq \alpha_0(1+\beta_0), \quad \forall j \text{ such that } c_j \in B_0 \\ & \quad \alpha_1(1-\gamma_1) \leq A_j x \leq \alpha_1(1+\beta_1), \quad \forall j \text{ such that } c_j \in B_j \end{aligned} \quad (13)$$

The required values are specified in Table 4.

Table 3. Pivotal rates in the part at risk.

| Number of organs (k) | | A_k | U_k | Q_k | $ B_k $ |
|--------------------------|---|-------|-------|-------|---------|
| B2 | 2 | 3.0 | 34 | 36 | 5750 |

| | | | | | |
|-----------|---|-----|----|----|--------|
| B3 | 3 | 2.0 | 30 | 42 | 3653 |
| B4 | 4 | 2.0 | 37 | 42 | 4200 |
| B5 | 5 | 1.1 | 25 | 35 | 200378 |
| B6 | 6 | 3.0 | 35 | 42 | 2351 |

Table 4. Pivotal rates in tumor tissues.

| | Number of organs (k) | α_k | β_k | γ_k |
|-------------------------|--------------------------|------------|-----------|------------|
| Intention-tissue | 0 | 67 | 0.11 | 0.11 |
| Increase-tissue | 1 | 72 | 0.07 | 0.07 |

Table 5. Optimum values for D_k and recommended constraints for approximations of

Also, Y_N is non-dominated set.

| k | $\min_{\{t y_t \in Y_N\}} D_k(\hat{x}^t)$ | $\max_{\{t y_t \in Y_N\}} D_k(\hat{x}^t)$ | U_k | Q_k |
|----------|---|---|-------|-------|
| 2 | 33.71 | 36 | 34 | 36 |
| 3 | 40.35 | 41 | 30 | 41 |
| 4 | 38.76 | 42 | 37 | 42 |
| 5 | 14.12 | 14.57 | 25 | 35 |
| 6 | 34.69 | 42 | 35 | 42 |

The application of the proposed method to the above HCM problem leads to the following results (see Figure.13).

Finally, the smallest and topmost even dose rate D_k in the part B_k $k = 2, \dots, 6$ can be compared over the total of approximation points as seen in Table 3.

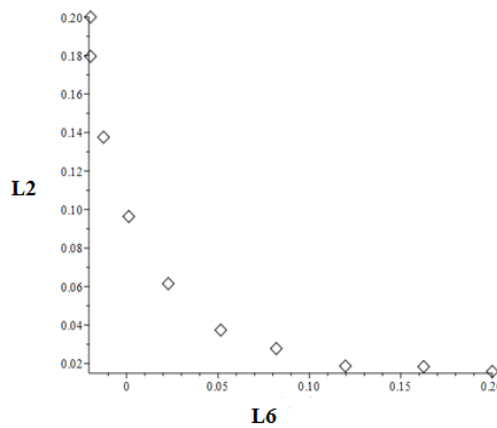


Figure 13. NDPs of the bi-objective HCM problem with the QND method

According to the above-mentioned approximations, the therapist can select an appropriate plan in which he can weigh the damage to the bladder and the rectum against each other.

Conclusions

In this paper, an efficient numerical method for solving MCOPs based on PS scalarization has been presented. The method produces a fine representation of the whole NDF for MCOPs. The introduced approach was applied to two problems and performed very well in terms of constructing the NDF. The algorithm was also applied to a HCM case study problem to demonstrate its applicability in practical problems.

In the current study, an optimized treatment plan for radiating a cancer tumor has been proposed. In this plan, besides getting rid of or weakening the cancer tumor, the least possible hazards and damages to the healthy organs of the body have been witnessed. Moreover, an optimized medicine plan for utmost impact on control and overcoming cancer tumors around healthy body organs is necessary.

Use of high doses of radiation leads to the side-effects in rectum and bladder, which is due to the high-range medicine pull of these organs. In the current study, minimizing the medicine pull in the bladder and the rectum was an aim. For this, a treatment plan is achieved by the physician in which the least suffering will happen in the patients' bladder and the rectum during the treatment process.

In the section on numerical examples, the results of the simulations showed that the time of performing the NC method was less than the mNBI and QND methods, which is due to the structure of the NC method, which is based on limiting the search space for the answer; this is contrary to the mNBI and QND methods that are gradient-oriented and do not limit the solution search space. As a result, it seems obvious that the computational complication of the NC approach is not worse than those of the other two approaches. On the other hand, the main criterion in the quality of NDP is its quality; examining the numbers in Tables 1 through 5 shows the superiority of the QND method. This indicates that the QND method has produced more high-quality responses than the other two methods, which firstly present a greater and better spread of the NDF, and secondly the distribution of responses is closer to the uniform distribution and can satisfy the demand of the decision-maker at any desired level. The results of the numerical simulations indicate that most of the QND solutions are superior to the solutions obtained from the other two methods and overcome them often. This

suggests that the QND method approximates the NDF with more details and less error compared with the other two methods. Along with all the qualities of the QND method, one of the disadvantages of it is the nonlinear structure of the method that leads to an increase in the computational complexity observed in the examples.

References

- Abo-Sinna, M., Abo-Elnaga, Y. Y., and Mousa, A. (2014). An interactive dynamic approach based on hybrid swarm optimization for solving multiobjective programming problem with fuzzy parameters. *Applied Mathematical Modelling*, 38(7-8), 2000-2014.
- Alber, M., and Reemtsen, R. (2007). Intensity modulated radiotherapy treatment planning by use of a barrier-penalty multiplier method. *Optimisation Methods and Software*, 22(3), 391-411.
- Audet, C., Savard, G., and Zghal, W. (2008). Multiobjective optimization through a series of single-objective formulations. *SIAM Journal on Optimization*, 19(1), 188-210.
- Brahme, A. (1984). Dosimetric precision requirements in radiation therapy. *Acta Radiologica: Oncology*, 23(5), 379-391.
- Cotrutz, C., Lahanas, M., Kappas, C., and Baltas, D. (2001). A multiobjective gradient-based dose optimization algorithm for external beam conformal radiotherapy. *Physics in Medicine and Biology*, 46(8), 2161.
- Craft, D., Halabi, T., Shih, H. A., and Bortfeld, T. (2007). An approach for practical multiobjective IMRT treatment planning. *International journal of radiation oncology* Biology* Physics*, 69(5), 1600-1607.
- Deb, K. (2001). *Multi-objective optimization using evolutionary algorithms* (Vol. 16). John Wiley and Sons.
- Ehrgott, M., and Burjony, M. (2001). *Radiation therapy planning by multicriteria optimization*. In *Proceedings of the 36th Annual Conference of the Operational Research Society of New Zealand* (pp. 244-253).
- Eichfelder, G. (2008). *Adaptive scalarization methods in multiobjective optimization* (Vol. 436). Berlin: Springer.
- Eichfelder, G. (2009). Scalarizations for adaptively solving multi-objective optimization problems. *Computational Optimization and Applications*, 44(2), 249.
- Eichfelder, G. (2014). Vector optimization in medical engineering *Mathematics Without Boundaries* (pp. 181-215). Springer, New York, NY.
- Kasimbeyli, R., Ozturk, Z. K., Kasimbeyli, N., Yalcin, G. D., and Erdem, B. I. (2017). Comparison of Some Scalarization Methods

- in Multiobjective Optimization. *Bulletin of the Malaysian Mathematical Sciences Society*, 1-31.
- Küfer, K.-H., Scherrer, A., Monz, M., Alonso, F., Trinka, H., Bortfeld, T., and Thieke, C. (2003). Intensity-modulated radiotherapy—a large scale multi-criteria programming problem. *OR spectrum*, 25(2), 223-249.
- Lopez, R. H., Rittob, T., Sampaio, R., and de Cursid, J. E. S. (2013). A new multiobjective optimization algorithm for nonconvex pareto fronts and objective functions. *Asociación Argentina de Mecánica Computacional*, 669-679.
- Meng, H.-y., Zhang, X.-h., and Liu, S.-y. (2005). In *International Conference on Natural Computation* (pp. 1044-1048). Springer, Berlin, Heidelberg.
- Messac, A., Ismail-Yahaya, A., and Mattson, C. A. (2003). The normalized normal constraint method for generating the Pareto frontier. *Structural and Multidisciplinary Optimization*, 25(2), 86-98.
- Messac, A., and Mattson, C. A. (2004). Normal constraint method with guarantee of even representation of complete Pareto frontier. *AIAA journal*, 42(10), 2101-2111.
- Niemierko, A. (1997). Reporting and analyzing dose distributions: a concept of equivalent uniform dose. *Medical physics*, 24(1), 103-110.
- Pardalos, P. M., Žilinskas, A., and Žilinskas, J. (2017). *Non-convex multi-objective optimization*. Springer International Publishing.
- Pintér, J. D., Linder, D., and Chin, P. (2006). Global Optimization Toolbox for Maple: An introduction with illustrative applications. *Optimisation Methods and Software*, 21(4), 565-582.
- Shukla, P. K. (2007). *On the normal boundary intersection method for generation of efficient front*. In *International Conference on Computational Science* (pp. 310-317). Springer, Berlin, Heidelberg.
- Siddiqui, S., Azarm, S., and Gabriel, S. (2011). A modified Benders decomposition method for efficient robust optimization under interval uncertainty. *Structural and Multidisciplinary Optimization*, 44(2), 259-275.
- Uilhoorn, F. E. (2017). Comparison of Bayesian estimation methods for modeling flow transients in gas pipelines. *Journal of Natural Gas Science and Engineering*, 38:159–170.
- Valipour, E., Yaghoobi, M., and Mashinchi, M. (2014). An iterative

- approach to solve multiobjective linear fractional programming problems. *Applied Mathematical Modelling*, 38(1), 38-49.
- Zhang, Q., Zhou, A., Zhao, S., Suganthan, P. N., Liu, W., and Tiwari, S. (2008). Multiobjective optimization test instances for the CEC 2009 special session and competition. *University of Essex, Colchester, UK and Nanyang technological University, Singapore, special session on performance assessment of multi-objective optimization algorithms.*